Water vapor line parameters and atmospheric transmittance in the 0.69 μm region

B.A. Voronin, S.S. Voronina, Yu.V. Voronina, and N.N. Lavrent'eva

Institute of Atmospheric Optics,
Siberian Branch of the Russian Academy of Sciences, Tomsk

Received September 8, 2004

A new database is presented for the 14395–14407 cm^{-1} region for calculations of the atmospheric transmission using the exact calculated line parameters. The semi-empiric approach developed has been used for calculation of the line broadening by air pressure and shifting coefficients of H_2O spectral lines, as well as the coefficients of thermal dependence of the line profile parameters. These calculations have been performed for 24 strongest lines. Four lines were assigned, and the atmospheric transmittance at the zenith angles of 70 and 80° has been simulated for the spectral range of a ruby laser.

Introduction

This work is a continuation of our previous research,[1–4] in which we estimated the contribution that comes to absorption of the solar radiation from weak absorption lines of water vapor, that are missing in the current HITRAN[5] and GEISA[6] databanks.

In this study we have investigated the molecular absorption in the range of 14395–14407 cm^{-1}, which is of interest for atmospheric applications, for example, for measurements of the concentrations of H_2O or O_2 with the use of a ruby laser radiation. For this spectral region, the presence of some substance in the atmosphere, that causes an excess absorption, was mentioned.[7] A part of this excess absorption can likely be assigned to absorption by weak water vapor lines, which are missing in the databanks. Therefore, the detailed information is a necessary condition for accurate calculations of the atmospheric transmission by the Earth's atmosphere in the region near 0.69 μm. This information includes, first of all, accurate line positions and intensities, quantum assignment of lines, air pressure broadening and self-broadening, shifting of the line position and the coefficient of temperature dependence for the line profile parameters.

Despite the HITRAN databank, including its latest versions, is the most complete and up-to-date database of spectra of atmospheric gases, it is not free of disadvantages. For example, as was noted in Ref. 8, there are mistakes in the HITRAN databank, resulting from compilation of spectra from original papers. Some spectral line parameters are lacking, or only average values are presented. In Ref. 9 it was demonstrated that one should use the averaged values of air broadening with care, because this can lead to significant errors (up to 100%) in considering the atmospheric absorption by weak H_2O absorption lines. For this reason in this study we have performed exact calculations of the air broadening coefficients for water vapor absorption lines.

Weak water vapor absorption lines, missing in the HITRAN-2000 databank, were taken from the Partridge–Schwenke *ab initio* calculations.[11] Our previous investigations, for example, in Ref. 10, showed that the calculations in Ref. 11 had high accuracy for line positions and a satisfactory one for line intensities. Therefore, the Partridge–Schwenke data can be used for atmospheric applications.

The positions and intensities of H_2O absorption lines for this region, included in the HITRAN-2000 databank, were taken from Ref. 12, which presents the absorption at the line peak for all transitions, and the intensities, along with their errors, only for 8 strongest lines lying in this region. The HITRAN-2000 contains also the information about the accuracy of line positions and halfwidths. The data on the accuracy of line positions and the error codes in the HITRAN coincide with those presented in Ref. 12. But for the errors in intensities, the situation is quite different. The highest accuracy in the intensities of transitions (from 1 to 2%) assigned to the four weakest lines, which even have no assigned positions in the databank, while for the strong lines the accuracy is either not determined or worse than 20%, whereas it is about 5% according to the data from Ref. 12. These remarks also were among the motivations of our investigation.

Technique and details of calculation of the line broadening and shift parameters

For compilation of the database on halfwidths and air pressure induced shifts of water vapor absorption lines, we used a semi-empiric technique, including various corrections associated with the deviation from the Anderson approximation.[13,14]

Within the framework of the semiclassical line broadening theory, the halfwidth γ_{if} and shift δ_{if}, attributed to the transition $i \to f$, can be written as

$$\gamma_{if} + i\delta_{if} = \frac{n}{c}\sum_k \rho(k) \int_0^\infty v f(v) dv \int_0^\infty \{U(i,f,k,b,v)\} b db, \quad (1)$$

the efficiency function $U(i, f, k, b, v)$ is

0235-6880/04/12 952-06 $02.00

$$\mathrm{Re}\{U(i,f,k,b,v)\} =$$

$$= 1 - \{1 - S^{(\mathrm{L})}_{2,fk,ik}\}\cos[S_{1,fk} - S_{1,ik} + \mathrm{Im}\{S_{2,fk}\} - \mathrm{Im}\{S_{2,ik}\}]\times$$

$$\times\exp[-(\mathrm{Re}\{S_{2,fk}\} + \mathrm{Re}\{S_{2,ik}\} + S^{(\mathrm{C})}_{2,fk,ik})]; \qquad (2)$$

$$\mathrm{Im}\{U(i,f,k,b,v)\} =$$

$$= \{1 - S^{(\mathrm{L})}_{2,fk,ik}\}\sin[S_{1,fk} - S_{1,ik} + \mathrm{Im}\{S_{2,fk}\} - \mathrm{Im}\{S_{2,ik}\}]\times$$

$$\times\exp[-(\mathrm{Re}\{S_{2,fk}\} + \mathrm{Re}\{S_{2,ik}\} + S^{(\mathrm{C})}_{2,fk,ik})],$$

where n is the number density of the buffer molecules; $\rho(k)$ is the population of the k level, k is the set of quantum numbers of the buffer molecule; v is the relative velocity of the colliding molecules; $f(v)$ is the Boltzmann distribution function; b is the impact parameter; S_1 and S_2 are the first- and second-order terms of the interaction efficiency function. The superscripts L and C refer to "linked" and "connected" diagrams of the perturbation theory. The first-order term S_1 is responsible for the adiabatic effect and is determined only by the isotropic part of the potential, while S_2 is determined by the anisotropic part. These two functions depend on the "classical" trajectory of relative motion of the colliding molecules.

Equations (1) and (2) represent the general formulation of the semiclassical theory. Their applicability depends on the approximations used for: a) the relative trajectory of the colliding molecules, b) intermolecular potential at both short and long distances, c) consideration of adiabatic and nonadiabatic effects, associated with the functions S_1 and S_2. In the Anderson theory, the relative motion is assumed rectilinear, and the intermolecular potential looks like a sum of contributions from long-range electrostatic forces.

In Ref. 15, Robert and Bonamy have developed a semiclassical (RB) theory, which uses a more realistic potential in the form of a sum of atom–atom short-range and electrostatic short-range potentials. They also used the effective parabolic trajectory in place of the rectilinear one. It was shown that the peculiarities of the intermolecular interaction at short distances and the bending of trajectories play an important role for close collisions, and the consideration of these factors significantly improves the calculations. Bykov et al.[16] proposed a model of exact trajectories (ET) for the semiclassical method of calculation of the broadening parameters. This model was successfully applied by Buldyreva et al. for calculating the line halfwidths.[17,18]

Different versions of the cut-off-free method, accounting for more and more finer effects, yielding small corrections, which were mentioned above, satisfactorily describe the H_2O line parameters, but, because of the complexity of calculations, they do not allow one to represent and analyze the processes, proceeding in the colliding molecules. Therefore, it is interesting to correct the Anderson method in order to remove its main disadvantages. In Ref. 19, we proposed some semiempirical version of such a correction. In this paper, it is considered with the equations for the halfwidth, taken as an example. The general equations (1) and (2) involve the transition probabilities $D^2(ii'|l)$ and $D^2(ff'|l)$ of different dissipation channels $i \to i'$, $f \to f'$, coupling the lower and upper transition levels with the neighboring levels. These parameters are the squared reduced matrix elements of the molecular operators, such as the dipole moment or components of the quadrupole tensor.

In the Anderson theory, the halfwidth can be expressed as a sum, including these parameters

$$\gamma_{if} = A(i,f) + \sum_l D^2(ii'|l)P_l^{\mathrm{A}}(\omega_{ii'}) +$$

$$+\sum_l D^2(ff'|l)P_l^{\mathrm{A}}(\omega_{ff'}) + \ldots \qquad (3)$$

with the higher-order terms neglected. Here $A(i, f) = \frac{n}{c}\sum_2 \rho(2)\int_0^\infty v\,\mathrm{d}v\,b_0^2(v,2,i,f)$ is the usual term of the Anderson theory, caused by the interruption ($b_0(v, 2, i, f)$ is the interruption parameter).

The sums in Eq. (3) include different-type transitions (dipole, quadrupole, etc.) and contain the products of two parameters $D^2(ii'|l)$ and $P_l^{\mathrm{A}}(\omega_{ii'})$. The transition strengths $D^2(ii'|l)$ and $D^2(ff'|l)$, attributed to the dissipation channels $i \to i'$, $f \to f'$, depend only on the properties of the absorbing molecule (dipole or quadrupole moments, wave functions) and include only intramolecular effects. The terms with $l = 1$ correspond to the dipole-type transitions, while $l = 2$ corresponds to the quadrupole transitions in the main molecule.

The parameters $P_l^{\mathrm{A}}(\omega_{ii'})$ can be considered as efficiency functions for this dissipation channel. $P_l^{\mathrm{A}}(\omega_{ii'})$ is a smooth function; therefore, it seems logical to introduce a correcting factor to this function, leaving without changes the term $D^2(ii'|l)$, describing the dynamics of the absorbing molecule, that is, to represent the efficiency functions $P_l^{\mathrm{A}}(\omega)$ in the form

$$P_l(\omega) = P_l^{\mathrm{A}}(\omega)[1 + a_1\omega + a_2\omega^2 + \ldots], \qquad (4)$$

where $P_l^{\mathrm{A}}(\omega)$ is the efficiency function in the Anderson approximation. The expression in the square brackets is the correction for different effects, ignored in the Anderson theory. The coefficients a_1, a_2 are determined from the fitting to the experimental values of the line broadening coefficients. The use of the efficiency function $P_l^{\mathrm{A}}(\omega)$ as the initial approximation in Eq. (4) allows the reconstruction of the correct behavior of halfwidths at the high values of the rotational quantum numbers or at high temperatures to be made. We used such a semi-empiric approach in Ref. 19, where it worked good in calculating the halfwidths and pressure caused shifts of CO_2 lines, giving good predictions even for a line with high J.

The calculation of nitrogen and oxygen pressure broadening of H_2O lines were performed with the use of the efficiency functions in the following form:

$$P_l(\omega_{ff'}) = P_l^{\mathrm{A}}(\omega_{ff'})[c_1/(c_2 + \sqrt{J_f})], \quad (5)$$

where c_1 and c_2 are the fitted parameters. Thus, we used a correcting factor to the function $P_l^{\mathrm{A}}(\omega)$ in the form of a simple expression, containing two parameters determined from the fitting to the experimental data. But this is not a simple operation of fitting to some experimental curve, because the correcting term, obtained from the fitting to several values of the broadening coefficients of some band, describes not only the experimental data in this band, but also the broadening and shift of lines for the whole set of bands of the colliding pair (in our case, H_2O–N_2).

The calculations of line halfwidths are performed taking into account the dipole–quadrupole interaction between the H_2O dipole moment and the quadrupole moment of the buffer molecule, as well as the quadrupole–quadrupole interactions.

The indices of the temperature dependence N' and N'' are determined as:

$$\gamma(T) = \gamma(300)\left(\frac{T}{300}\right)^{-N'}, \qquad \delta(T) = \delta(300)\left(\frac{T}{300}\right)^{-N''}. \quad (6)$$

Having calculated the coefficients of broadening and shift by nitrogen and oxygen as described above for temperatures of 200–350 K and used the equations

$$\gamma_{\mathrm{air}} = 0.79\gamma_{\mathrm{N_2}} + 0.21\gamma_{\mathrm{O_2}}, \qquad \delta_{\mathrm{air}} = 0.79\delta_{\mathrm{N_2}} + 0.21\delta_{\mathrm{O_2}}, \quad (7)$$

we obtain the corresponding air broadening and shift coefficients and the indices of their temperature dependence.

Parameters of the lines in the spectral range of a ruby laser emission

To compile a new database for the spectral range of a ruby laser emission, we used the HITRAN-2000 databank, the Partridge–Schwenke calculation,[11] and the available experimental data.[20,21] Among 17 of the $H_2{}^{16}O$ lines, included in HITRAN for this range, four lines are unassigned and the air-broadening and self-broadening coefficients for them are presented by averaged values. From the Partridge–Schwenke calculation,[11] we took only the lines with the intensity higher than 10^{-29} cm/mol.: 123 lines of $H_2{}^{16}O$, 68 lines of $H_2{}^{18}O$, and 27 lines of $H_2{}^{17}O$. The HDO lines with the intensity higher than 10^{-29} cm/mol. are absent in this region. For the seven strongest (with the intensity ~10^{-26} cm/mol.) lines from Ref. 11, missing in HITRAN, the line positions were refined using the upper and lower energy levels determined by processing the experimental spectra.[20,21] For the other weak lines, the refinement was made whenever it was possible in principle, that is, the lower energy levels were mostly refined. The four lines, unassigned in HITRAN, were assigned in accordance with Ref. 20. The broadening and shift parameters were calculated for 24 lines.

The Table presents the frequency, quantum rotational-vibrational assignment, and parameters of the lines for the 14395–14407 cm^{-1} range. The four lines, unassigned in HITRAN-2000, are presented with the index i, and their assignment is taken from Ref. 20. Seven lines marked by s are the strongest lines (with the intensity ~10^{-26} cm/mol.) from the Partridge–Schwenke calculation.[11] The positions of these seven lines are refined using the energy levels, determined from the analysis of the experimental spectra.[20,21] In addition, the Table presents the air broadening calculated in this work γ_{air} and the air broadening from HITRAN-2000 $\gamma_{\mathrm{air}}(\mathrm{H})$. The coefficient γ_{air} from HITRAN for the lines 14395.9407, 14397.6187, 14397.9000, and 14406.9532 is tabulated equal to 0.0964 cm^{-1}/atm, but our calculation shows that for the line 14397.6187 it is halved and equals to 0.05433 cm^{-1}/atm. For the lines 14395.9407, 14397.9000, and 14406.9532, γ_{air} differs not so widely and is equal to 0.08747, 0.09240, and 0.09450, respectively. The data on self-broadening γ_{self} are taken from HIRTAN. For the lines marked by the asterisk (*), the data on γ_{self} were absent, and our approximate calculation – averaging over the J-dependence – is presented. The temperature dependence δ, and the coefficients n_γ, $n_\gamma(\mathrm{H})$, and n_δ were then calculated. In addition, the Table gives the line intensities from the Partridge–Schwenke calculation $I(\mathrm{S})$ and from HITRAN-2000 $I(\mathrm{H})$, as well as the upper E' and lower E'' energy levels. One upper level, marked by s, was taken from Ref. 11, two levels, marked by t, were taken from Ref. 21, and the other upper levels from Ref. 20.

Description of the method for transmittance calculation and results of simulation

The transmittance was calculated by the line-by-line method, which accounts for the contribution coming from every line to the absorption at a given frequency. The transmission function was described by the equation

$$T_{\Delta\nu} = \frac{1}{\nu}\int_{\Delta\nu}\exp[-\tau(\nu)]\mathrm{d}\nu, \quad (8)$$

where

$$\tau(\nu) = \frac{1}{\cos\varphi}\int_{z_2}^{z_1}\sum_{i=1}^{N}k_i(\nu,z)\rho(z)\,\mathrm{d}z \quad (9)$$

is the optical depth; N is the number of lines taken into account; φ is the zenith angle; $k_i(\nu, z)$ is the absorption coefficient of the ith line, determined for the unit concentration of the absorbing gas; $\rho(z)$ is the concentration of the absorbing gas at the height z.

Water vapor lines in the spectral region of a ruby laser emission

ν	$v_1\,v_2\,v_3$	$J'\;K'_a\,K'_c$	$J''\;K''_a\,K''_c$	γ_{air}	γ_{air}(H)	γ_{self}(H)	δ	n_γ	n_γ(H)	n_δ	I(S)	I(H)	E'	E''
14395.3028	0 0 4	5 0 5	6 1 6	0.07534	0.0737	0.4338	−0.02183	0.378	0.75	1.323	$2.15\cdot10^{-26}$	$4.46\cdot10^{-26}$	14842.5552	447.2524
14395.9407*i*	1 0 3	3 3 1	3 1 2	0.08747	0.0964	0.4545	−0.01105	0.635	0.68	0.603	$4.13\cdot10^{-26}$	$1.40\cdot10^{-26}$	14569.3065	173.3658
14396.1431	1 0 3	8 5 3	7 5 2	0.06505	0.0644	0.3841	−0.02359	0.452	0.68	0.980	$8.03\cdot10^{-26}$	$5.92\cdot10^{-26}$	15455.9791	1059.836
14396.4570*s*	2 4 0	8 8 1	7 5 2	0.05020	—	0.317*	−0.04493	0.318	—	1.356	$1.86\cdot10^{-26}$	—	15456.2930*s*	1059.836
14397.3635	1 0 3	5 1 5	4 1 4	0.08230	0.0812	0.4430	−0.01651	0.491	0.61	1.121	$8.41\cdot10^{-24}$	$4.89\cdot10^{-24}$	14622.2019	224.8384
14397.5811*s*	1 0 3	8 2 7	8 0 8	0.05446	—	0.317*	−0.03929	0.113	—	1.545	$1.68\cdot10^{-26}$	—	15141.6448	744.0637
14397.6187*i*	1 0 3	8 1 7	8 1 8	0.05433	0.0964	0.4545	−0.03837	0.148	0.68	1.588	$5.10\cdot10^{-26}$	$6.21\cdot10^{-26}$	15141.7814	744.1627
14397.9000*i*	0 0 4	2 1 2	3 2 1	0.09240	0.0964	0.4545	−0.01654	0.713	0.68	0.779	$1.73\cdot10^{-26}$	$3.37\cdot10^{-26}$	14610.0564	212.1564
14400.0730	4 0 0	6 4 2	5 3 3	0.07611	0.0741	0.3859	−0.01809	0.572	0.68	0.894	$1.68\cdot10^{-25}$	$1.07\cdot10^{-25}$	14904.0411	503.9681
14400.2409*s*	4 0 0	6 4 3	5 3 2	0.07835	—	0.443*	−0.01769	0.630	—	0.900	$2.26\cdot10^{-26}$	—	14909.0530	508.8121
14400.3285	1 0 3	5 0 5	4 0 4	0.08482	0.0837	0.4400	−0.01478	0.547	0.68	0.981	$3.09\cdot10^{-24}$	$1.89\cdot10^{-24}$	14622.3812	222.0527
14400.7314*s*	0 0 4	3 1 2	4 2 3	0.09078	—	0.563*	−0.01593	0.638	—	0.870	$2.27\cdot10^{-26}$	—	14701.0937	300.3623
14400.7819	1 0 3	4 2 2	3 2 1	0.08823	0.0915	0.4400	−0.01406	0.683	0.68	0.774	$6.20\cdot10^{-24}$	$3.60\cdot10^{-24}$	14612.9383	212.1564
14402.4341	1 0 3	7 4 4	6 4 3	0.07032	0.0710	0.4040	−0.02287	0.457	0.68	1.089	$3.47\cdot10^{-25}$	$2.19\cdot10^{-25}$	15159.1590	756.7249
14402.7474	1 0 3	5 3 3	4 3 2	0.07578	0.0788	0.3890	−0.01903	0.543	0.54	1.034	$2.61\cdot10^{-24}$	$1.76\cdot10^{-24}$	14785.2643	382.5169
14403.1693*s*	1 0 3	9 5 5	8 5 4	0.06078	—	0.309*	−0.02728	0.342	—	1.201	$3.10\cdot10^{-26}$	—	15658.3363*t*	1255.167
14403.1818*s*	4 0 0	5 5 1	4 4 0	0.05213	—	0.495*	−0.03438	0.402	—	1.197	$1.94\cdot10^{-25}$	—	14891.3160	488.1342
14403.1819	4 0 0	5 5 0	4 4 1	0.05189	0.0513	0.2975	−0.03449	0.395	0.68	1.199	$5.77\cdot10^{-25}$	$6.83\cdot10^{-25}$	14891.2912*t*	488.1077
14403.4766*s*	1 0 3	9 2 8	9 0 9	0.04559	—	0.309*	−0.04944	0.063	—	1.541	$1.80\cdot10^{-26}$	—	15323.6451	920.1685
14404.8663	1 0 3	4 1 3	3 1 2	0.09177	0.0922	0.4870	−0.01405	0.678	0.68	0.778	$8.84\cdot10^{-24}$	$5.12\cdot10^{-24}$	14578.2321	173.3658
14405.7822	1 0 3	5 3 2	4 3 1	0.08061	0.0939	0.4840	−0.01636	0.681	0.68	0.784	$9.58\cdot10^{-25}$	$6.06\cdot10^{-25}$	14789.6247	383.8425
14406.0515	1 0 3	5 2 4	4 2 3	0.08087	0.0844	0.4389	−0.01742	0.517	0.68	1.102	$5.45\cdot10^{-24}$	$3.34\cdot10^{-24}$	14706.4138	300.3623
14406.7745	1 0 3	7 4 3	6 4 2	0.07880	0.0710	0.4228	−0.01815	0.635	0.68	0.745	$9.49\cdot10^{-26}$	$5.76\cdot10^{-26}$	15164.5547	757.7802
14406.9532*i*	4 0 0	3 3 1	2 0 2	0.09450	0.0964	0.4545	−0.00525	0.645	0.68	−0.536	$2.57\cdot10^{-26}$	$2.24\cdot10^{-26}$	14477.0440	70.09079

N o t e s : ν is frequency, in cm^{-1}; $v_1\,v_2\,v_3$ are upper vibrational quantum numbers; $J\,K_a\,K_c$ are upper and lower rotational quantum numbers; γ_{air} is the air broadening coefficient, in cm^{-1}/atm (296 K); γ_{self}(H) is the self-broadening coefficient, cm^{-1}/atm (296 K) (* marks the J-dependence); δ is the pressure-induced shift coefficient, cm^{-1}/atm (296 K); n_γ is the coefficient of the temperature dependence of halfwidth; n_δ is the coefficient of the temperature dependence of shift; I(S) is the intensity, $cm^{-1}/(mol\cdot cm^{-2})$, 296 K, from the calculation[5]; I(H) is the intensity, $cm^{-1}/(mol\cdot cm^{-2})$, 296 K, from HITRAN-2000; E' (E'') are upper (lower) energy levels, cm^{-1}; (H) denotes HITRAN-2000; (S) denotes the Partridge–Schwenke calculation.

In this calculation, we used the Voigt profile. Only the absorption by water vapor and its continuum absorption (CKD 2.4 model) were taken into account. The transmittance was calculated for the zenith angles of 70 and 80°.

Three series of model calculations were performed to analyze the effect from refinement of the HITRAN databank on the basis of the Partridge–Schwenke data and our data on the halfwidths. The results calculated by modeling are shown in Figs. 1–4. Figure 1 shows the effect of corrected air broadening coefficients on the results calculated.

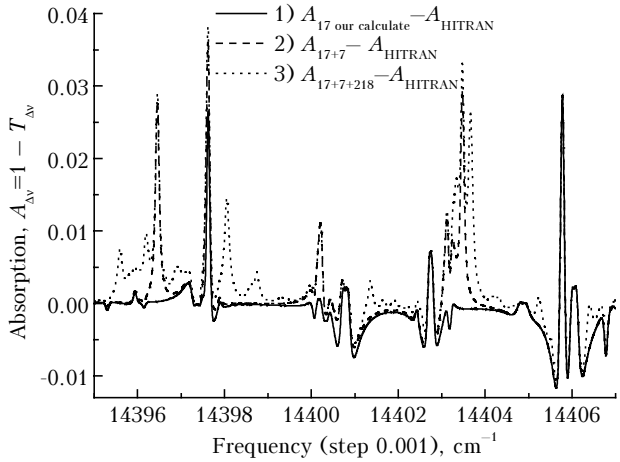

Fig. 1. Difference in the absorption when accounting for different number of lines at the zenith angle of 70°.

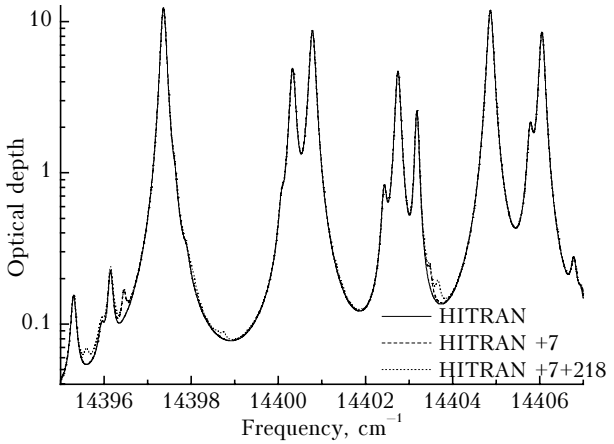

Fig. 2. Simulation of optical depth for the zenith angle of 80°.

The curves in Figs. 1–4 show the following:

1) The solid curve shows the difference between the calculated absorption for 17 lines from HITRAN-2000 with the air broadening coefficients changed in accordance with our calculations (see the Table) and for the same lines but with unchanged coefficients. That is, this curve shows the difference due to only the refinement of the air broadening coefficients for the H_2O absorption lines.

2) The dashed curve shows the difference between the absorption for 17 lines from HITRAN-2000 and the same lines with the changed parameters, as well as the additional seven strongest lines from the Partridge–Schwenke calculation[11] (these lines are marked by the asterisk in the Table).

3) The dotted curve shows the difference between the absorption in 17 typical lines from HITRAN-2000 and the same lines with the changed broadening parameters and the additional seven strong and 218 weak lines from the Partridge–Schwenke calculation.[11]

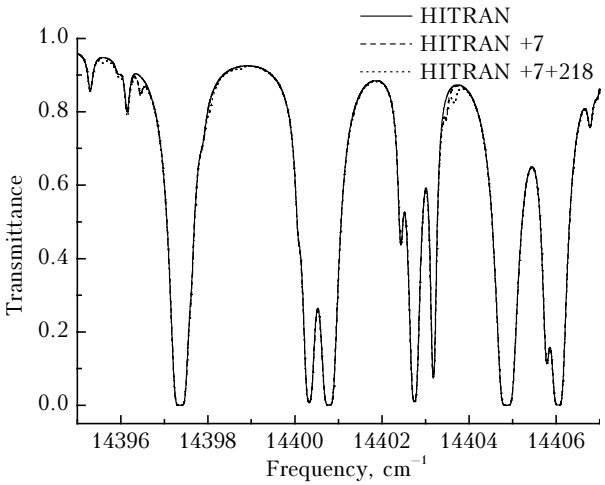

Fig. 3. H_2O transmittance in the 14395–14407 cm^{-1} region for the zenith angle of 80°.

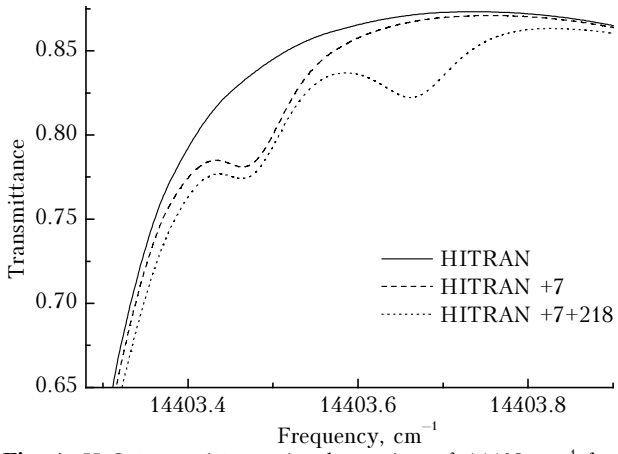

Fig. 4. H_2O transmittance in the region of 14403 cm^{-1} for the zenith angle of 80°.

The difference between the calculations for the first and second cases in Fig. 1 gives 3% in absorption, which is already a significant value, because the typical error in determination of the absorption function for the Fourier transform spectrometers is about 1% and smaller (that is, the signal-to-noise ratio ~ 100/1 and higher[22]). For the third case, when all possible lines with the intensities from the Partridge–Schwenke calculation[11] are taken into account, the difference is already as high as 4%, which is indicative of the need in additional information about weak lines and/or continuum absorption of water vapor.[7]

Figure 2 shows the calculated optical depth for the three situations described above. In the first case, the absorption by 17 lines from HITRAN-2000 is shown by the solid curve (17 lines in this region and 62 neighboring lines, lying in the 13370–14432 cm^{-1} region, which are taken into account by far wings). In the second case (dashed curve), 17 lines from HITRAN-2000 are supplemented with seven strongest $H_2{}^{16}O$ lines from the Partridge–Schwenke calculation.[11] The positions of these seven lines were refined from the known experimental upper energy levels.[20,21] In the third case (dotted curve), 17 and 7 lines are supplemented with 218 lines from the Partridge–Schwenke calculation,[11] corresponding to the isotopic modifications of $H_2{}^{16}O$, $H_2{}^{17}O$, and $H_2{}^{18}O$.

Figure 3 depicts the transmittance in the spectral region of 14395–14407 cm^{-1} for conditions described above for Fig. 2. It can be seen that the missing lines can contribute significantly nearby 14396 and 14404 cm^{-1}. Figure 4 shows the transmittance near 14404 cm^{-1}. It can be seen from Fig. 4 that the contribution of the missing absorption lines differs by almost 7% from the calculation based on the HITRAN data bank.

Conclusions

This paper presents the most complete up-to-date information on the spectral line parameters of water vapor in the 14395–14407 cm^{-1} region.

It is shown that the HITRAN uses the averaged air broadening coefficients for some water vapor lines and their refinement can lead to a significant, up to 3%, increase of the absorption at long paths through the atmosphere at a zenith angle of 70°.

The account of all water vapor absorption lines,[11] missing in HITRAN, can contribute up to 5–7% to the absorption (the path at a zenith angle of 80°).

Supplementing the HITRAN-2000 database with the strongest water vapor absorption lines from the Partridge–Schwenke calculation,[11] we can increase the absorption by 3–5%. It should be expected that the additional lines could be recorded experimentally in the spectrum with the use of, for example, photoacoustic instrumentation.[7,23]

Acknowledgments

The authors are grateful to S.D. Tvorogov, A.D. Bykov, and K.M. Firsov for fruitful discussions.

This work was supported, in part, by the Russian Foundation for Basic Research (Grant No. 04–05–64569a), The Division of Physical Sciences of the RAS (Grant No. 2.10), and the Ministry of Education (2002) (Grant E02–3.2–91).

References

1. A.D. Bykov, B.A. Voronin, O.V. Naumenko, L.N. Sinitsa, K.M. Firsov, and T.Yu. Chesnokova, Atmos. Oceanic Opt. **12**, No. 9, 755–757 (1999).
2. B.A. Voronin, A.B. Serebrennikov, and T.Yu. Chesnokova, Atmos. Oceanic Opt. **14**, No. 9, 718–721 (2001).
3. B.A. Voronin and S.S. Voronina, Atmos. Oceanic Opt. **15**, No. 4, 321–324 (2002).
4. B.A. Voronin, I.M. Nasretdinov, A.B. Serebrennikov, and T.Yu. Chesnokova, Atmos. Oceanic Opt. **16**, No. 3, 272–276 (2003).
5. http://www.hitran.com
6. http://ara.lmd.polytechnique.fr
7. B.A. Tikhomirov, A.B. Tikhomirov, and K.M. Firsov, Atmos. Oceanic Opt. **14**, No. 9, 674–680 (2001).
8. L.P. Giver, C. Chackerian, Jr., and P. Varanasi, J. Quant. Spectrosc. Radiat. Transfer **66**, 101–105 (2000).
9. I.V. Ptashnik and K.P. Shine, Atmos. Oceanic Opt. **16**, No. 3, 251–255 (2003).
10. B.A. Voronin, Izv. Vyssh. Uchebn. Zaved., Fiz., No. 3, 93–100 (1999).
11. H. Partridge and D. Schwenke, J. Chem. Phys. **106**, No. 11, 4618–4639 (1997).
12. J.-Y. Mandin, C. Camy-Peyret, J.-M. Flaud, J.-P. Chevillard, and J.W. Brault, J. Mol. Spectrosc. **116**, 167–190 (1986).
13. P.W. Anderson, Phys. Rev. **76**, 657–661 (1949).
14. C.J. Tsao and B. Curnutte, J. Quant. Spectrosc. Radiat. Transfer **2**, 41–91 (1961).
15. D. Robert and J. Bonamy, J. de Phys. **40**, No. 10, 923–943 (1979).
16. A.D. Bykov, N.N. Lavrent'eva, and L.N. Sinitsa, Atmos. Oceanic Opt. **5**, No. 9, 587–594 (1992).
17. J. Buldyreva, J.J. Bonamy, and D. Robert, J. Quant. Spectrosc. Radiat. Transfer **62**, 321–343 (1999).
18. J. Buldyreva, S. Benec'h, and M. Chrysos, Phys. Rev. A **63**, No. 1, 708–722 (2001).
19. A.D. Bykov, N.N. Lavrent'eva, and L.N. Sinitsa, Atmos. Oceanic Opt. **13**, No. 12, 1015–1019 (2000).
20. A. Bykov, O. Naumenko, L. Sinitsa, B.A. Voronin, J.-M. Flaud, C. Camy-Peyret, and J.-Y. Mandin, Proc. SPIE **3583**, 119–124 (1998).
21. J. Tennyson, N.F. Zobov, R. Williamson, O.L. Polyansky, and P.F. Bernath, J. Chem. Phys. **106**, No. 11, 4618–4639 (1997).
22. R.A. Toth, J. Mol. Spectrosc. **186**, 66–89 (1997).
23. A.B. Tikhomirov and B.A. Tikhomirov, in: *Abstracts of Reports at XI Joint International Symposium on Atmospheric Physics,* IAO SB RAS, Tomsk (2004), A1-22, p. 52.